

Modeling of Electric Arc Furnaces (EAF) with electromagnetic stirring

Ola Widlund¹, Ulf Sand², Olof Hjortstam², Xiaojing Zhang¹

¹ ABB AB, Corporate Research
Forskargränd 7
SE-721 78
Västerås, Sweden

² ABB AB, Metallurgy
Terminalvägen 24
SE-721 59
Västerås, Sweden

Contact: Ola Widlund, e-mail: ola.widlund@se.abb.com

Keywords: Electric arc furnace, EAF, electromagnetic stirring, CFD, flow modeling

Abstract

Electromagnetic stirring can play an important role in modern Electric Arc Furnaces (EAF), as they often operate far from equilibrium conditions, with tap-to-tap times of 45 minutes or less, high electric power input and significant energy additions from fuel and oxygen. Numerical modeling is used extensively in ABB's current efforts to optimize the EAF process with electromagnetic stirring. The modeling approach uses a Finite-Element method (FEM) for computing the forces generated by the electromagnetic stirrer, whereas the resulting flow properties, heat and mass transfer in the system is computed using a Finite-Volume (FVM) flow solver. The paper presents the numerical model in greater detail and discusses some important results. We show that electromagnetic stirring gives a more than ten-fold increase of flow velocities and circulation, compared with a flow driven by natural convection alone. The global circulation created by electromagnetic stirring dramatically reduces temperature differences in the melt, thus reducing super-heating of the melt surface and risks for cold regions. Efficient mixing of chemical species, together with even temperatures, is beneficial for efficiency and controllability of the chemical reactions in the slag-metal interface.

Introduction

The Electric Arc Furnace (EAF) was historically the first application in the metallurgical industry to benefit from electromagnetic stirring. The technology was developed 70 years ago by ASEA (currently ABB), with the first commercial installation in 1947 at Uddeholm (Hagfors, Sweden). Focus was then on refining processes like alloying and homogenization.

In the last 40 years, new technologies have been applied into the EAF process, such as slag foaming, ultra-high power (UHP) and computerized monitoring. Different secondary technologies have also been developed, which leads to limited refining tasks remaining in the EAF.

However, modern EAF processes (with tap-to-tap times of 45 minutes or less) operate far from equilibrium, with significant energy addition from oxygen and fuel. Therefore electromagnetic stirring can play an important role in the state-of-the-art EAF process.

During scrap melting, stirring can make the process more robust and less sensitive to larger scrap pieces.

Stirring of the melt will give a more homogeneous distribution of temperature and chemical composition and improved slag/metal reaction. This reduces melt over-heat and super-saturation of oxygen, increasing iron yield and refractory life, with improvements in productivity and reduction of production costs and energy consumption. Electromagnetic stirring offers several advantages over traditional gas stirring, such as no extra down-time for maintenance, better global melt circulation and significantly improved work place safety.

Figure 1 is an illustration of a modern electric arc furnace with eccentric bottom tapping (EBT) and equipped with an electromagnetic stirrer.

ABB has developed a new family of electromagnetic stirrers, EAF-EMS, optimized for electric arc furnaces; see illustration in Figure 2. The core is bent to follow the bottom curvature of the furnace and give optimum penetration of forces into the melt.

In ABB's current efforts to optimize the EAF process further, numerical modeling has a prominent place. Building on solid experience from process modeling of electromagnetic stirring in many different metallurgical processes, we use a transient finite-

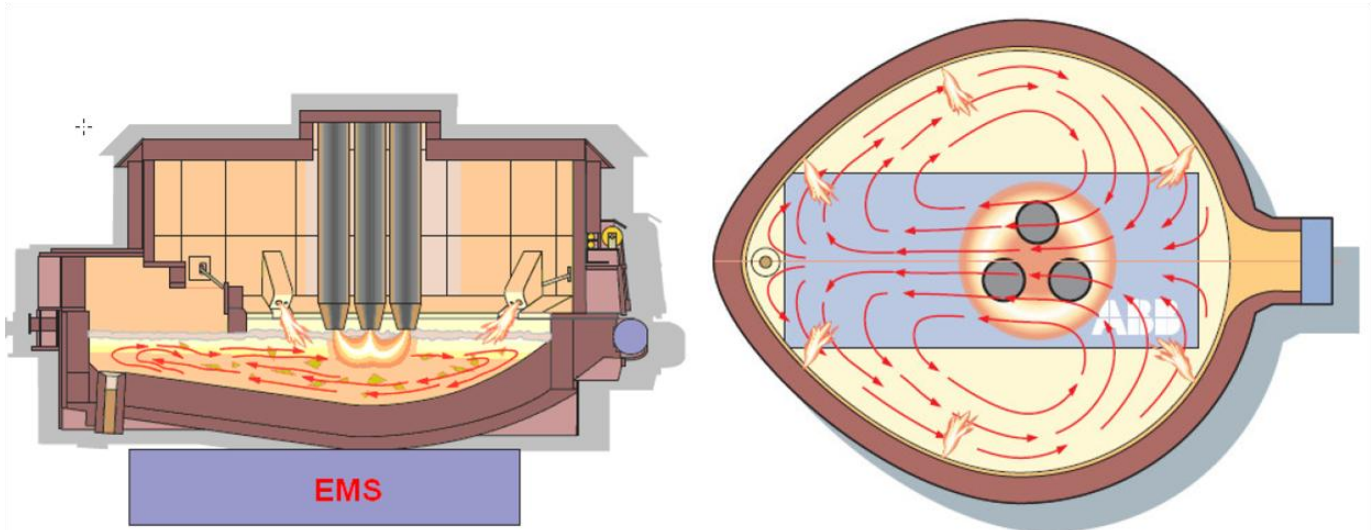


Figure 1: Illustration of a modern EBT-type electric arc furnace equipped with an electromagnetic stirrer (EMS).

volume CFD solver for the melt flow, convective and radiative heat transfer, melting of solids and species transport. The electromagnetic stirring forces are imported from a finite element-based electromagnetic simulation of the stirrer device. Modeling of the heat transfer is based on a detailed energy analysis of the process.

The results show that electromagnetic stirring can improve the EAF process and reduce the energy needed significantly.

Modeling objectives

Advanced simulation tools are routinely used within ABB for a wide range of metallurgical applications, to support electromagnetic stirrer design and predictions of performance in customer's processes. Process engineers can use parameterized models for highly automated standard simulations on a remote Linux cluster with comprehensive reporting of key performance indicators.

Scrap melting and conditioning in an electric arc furnace is a very complex batch operation, with several more or less distinct process steps. A complete numerical model of the whole batch process would be both difficult to develop and impractical to use for process engineering. Instead our objective is to develop several different model setups, addressing separate aspects of the process and the effects of stirring:

- Mixing efficiency
- Heat transfer and temperature distribution
- Prediction of wall shear (refractory wear)
- Melting of large scrap pieces and sculls on the furnace walls
- Reaction rates in the melt-slag interface (key reactions and yield)
- Motion of the slag during stirring

Where appropriate, the impact of electromagnetic stirring is assessed relative to the performance when the melt circulation is driven only by natural convection due the electric arc heating of the melt surface.

Numerical modeling approach

The numerical modeling uses commercial software for the electromagnetic design as well as the flow and heat transfer. The electromagnetic stirrer device and the furnace structure is modeled using the FEM software OPERA by Vector Fields Software, which computes the volumetric magnetic forces in the steel melt. These forces are then interpolated to the finite volume mesh used for modeling the flow and heat transfer with ANSYS FLUENT. The use of a similar workflow for modeling of electromagnetic stirring in ladle furnaces is described in greater detail in [2].



Figure 2: Model of novel ABB electromagnetic stirrer EAF-EMS, optimized for electric arc furnaces. The size of human is shown for comparison.

The FEM simulation computes the electromagnetic forces assuming the melt is stagnant. When using the forces inside ANSYS FLUENT we therefore apply a correction to compensate for the motion of the melt; in the horizontal stirring direction, y , we have

$$F_y = F_{0,y} \left(1 - \frac{v}{2f\tau} \right),$$

where v is the velocity component in the stirring direction, f is the stirrer frequency and τ is the pole pitch, i.e. the centre-to-centre distance between two magnetic poles.

The melt flow in the furnace is usually unsteady. To capture the true nature of the process, the flow and heat transfer simulation is therefore transient, with time steps in the order of 0.1 s. Mean properties of the flow are obtained by averaging over a few minutes of physical time, once the flow has developed beyond the startup transients.

We generally use the Reynolds Stress Transport (RST) model (with standard linear pressure-strain modeling) to model the turbulence. For the calculations presented in this paper, however, we have resorted to using the realizable K- ϵ model, due to problems getting robust solutions for the reference case with only natural convection (no stirring). The RST model is less robust than simpler two-equation models like the K- ϵ model, but the latter have a tendency to predict the flow as stable and steady-state, even when it is not. Full Reynolds stress models are also considered more accurate for flows with strong mean rotation.

Refractory walls are modeled with a thin-wall boundary condition available in FLUENT [1]. This avoids meshing of the solid and solving the complete conjugate heat transfer problem. The thin-wall boundary condition allows the specification of a wall thickness, with given material properties. The heat transfer across the boundary is governed by the thermal resistance of the wall material, together with specifications of a heat transfer coefficient (for convection), an emissivity coefficient (for radiation) and ambient temperature on the outside of the wall boundary. The major drawback of this simplified treatment of the walls is that the thermal inertia of the walls is neglected. The time response of the walls over the batch cycle is therefore not captured.

In the base model for the predictions of flow patterns, heat transfer and mixing efficiency, the liquid slag layer is currently not explicitly modeled, but represented with a thin-wall boundary condition similar to that used for the refractory walls. The convective heat transfer across the slag layer therefore cannot be represented correctly; we set the

thermal conductivity of this “slag boundary” to an artificially high value to somewhat compensate for this.

The heat from the arcs is represented by heat flux boundary conditions applied on circular patches on the melt surface, below the arcs. Although a simplification of the real mechanisms, this approach is common in the literature, see i.e. [3][4]. Only a fraction of the total electrical power is available to heat the melt, as significant amounts are lost to the freeboard, either directly by radiation from the arcs, or indirectly through heating of the slag layer.

In the absence of electromagnetic stirring, natural convection is the major mechanism driving the flow. It is modeled using the Boussinesq hypothesis, with which a linearized buoyancy force is expressed as

$$\vec{F}_b = -\vec{g}\rho_{\text{ref}}\beta(T - T_{\text{ref}}),$$

where ρ_{ref} is the density at the reference temperature T_{ref} , \vec{g} is the gravity vector and β is the volume expansion coefficient of the fluid. In the present paper, natural convection is included for consistency also when electromagnetic stirring is applied, although the effects of buoyancy are negligible compared to the electromagnetic forces.

A base model of the EAF has been developed to assess basic features like flow patterns, wall shear, temperature distribution and heat transfer, as well as the efficiency in mixing of trace species. The stirrer forces can be in the forward direction (towards the EBT region), or in the reverse direction, or it can be operated intermittently in both directions.

A variant of the basic flow and heat transfer model includes the possibility to define regions of solid material in the melt and use the melting and solidification model of ANSYS FLUENT to study how the melting of skulls and large pieces of scarp is accelerated by stirring.

A separate model is used for studying the redistribution of the slag layer and the deformation of the melt-slag interface due to stirring. The model uses a three-phase volume-of-fluid (VOF) representation of the melt, the slag and the air above. In this model we look only at the flow of melt and slag; arc heating and heat transfer is not considered.

Ongoing efforts address prediction of how stirring affects key chemical reactions. The chemistry in the system is controlled by equilibrium in the slag-metal interface and mass transfer of reacting species in slag and steel melt to the interface. A detailed description of the chemistry would require advanced chemical modeling and an accurate description of both the slag and the slag-metal interface. A simpler starting point is to predict and compare reaction rates

for key reactions from local flow properties like temperatures and species concentrations at the melt surface.

In the present paper we will present results from the base model, to discuss flow patterns, heat and mass transfer.

Reference case simulations

The reference case used for the examples in this paper is a hypothetical electric arc furnace with eccentric bottom tapping (EBT) and a melt content of 150 ton. The geometry is illustrated in Figure 3, with key design parameters summarized in Table 1. The mesh used for the flow simulation is a so-called cutcell, or “octree”, mesh with a nominal mesh size of 45 mm. Inflation layers are applied on all boundaries, resulting in a mesh with about 360 thousand cells. Figure 4 shows a cross-section through the mesh. Model parameters and physical properties are summarized in Table 2.

An arc furnace of this size would typically have a nominal arc power of 80-100 MW. Depending on operation and slag foaming practices, only part of this

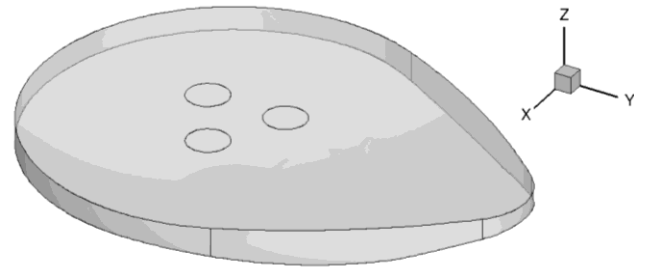


Figure 3: Arc furnace geometry. The circles on the top surface are the boundaries representing the arc impingement zones, where heat is injected.

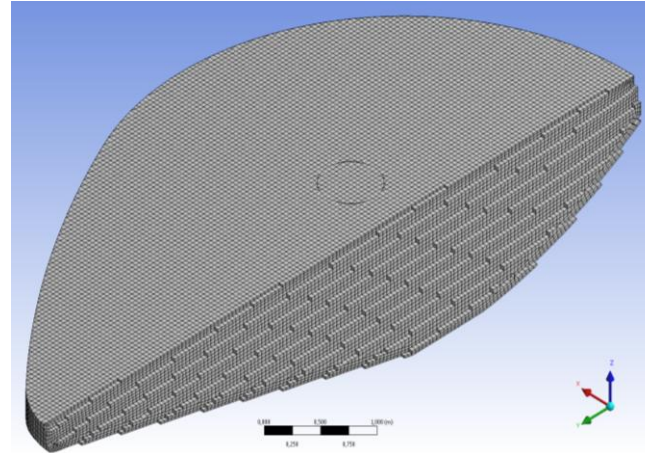


Figure 4: Mesh used in the flow simulations (melt only).

energy will be injected directly into the melt. For the example presented here we supply 50 MW of heat to the melt surface. The heat is injected in three arc impingement spots on the surface, using wall heat flux boundary conditions. However, in order to get robust convergence for the case of natural convection (no stirring) it was necessary to ramp up the power gradually. During this power ramp-up, a decreasing fraction of the heat was supplied as a volume source term in a shallow region (0.3 m) immediately below the arc impingement spots, to help establish a buoyancy-driven flow regime. The initial ramp-up phase lasts for 60 s; after this time, full power is supplied to the surface. For consistency, the same ramp-up is used also for the case with electromagnetic stirring.

The thin-wall boundary conditions applied on bottom and side walls use realistic values of refractory thickness and thermal properties. The results will show that the heat losses from these boundaries are relatively small.

For the thin-wall boundary representing the slag layer, we have estimated an effective value of the slag thermal conductivity which gives a realistic temperature (~1500 K) of the outside surface, i.e. the slag surface, which loses heat to the freeboard by radiation and convection. Depending on the

Design parameter	Value	Unit
Melt content	150	ton
Length	7.2	m
Large diameter (melt)	5.7	m
Diameter in EBT region	1.8	m
Melt height	1.15	m
Slag height	0.25	m
Thickness of side walls	0.40	m
Thickness of bottom wall	0.80	m
Electrode radial positions	0.675	m

Table 1: Design parameters for the melt volume of the reference case electric arc furnace.

Model parameter	Value	Unit
Melt density	6900	kg/m ³
Melt Cp	792	J/kg·K
Melt thermal conductivity	35	W/m·K
Melt viscosity	0.007	kg/m·s
Melt thermal expansion coeff.	0.0003	1/K
Slag thermal conductivity	80	W/m·K
Trace scalar mass diffusivity	1·10 ⁻⁵	m ² /s
Refractory thermal conductivity	0.5	W/m·K
Heat transfer coefficient, outside of bottom and side walls	10	W/m ² ·K
Ambient temperature	300	K
Freeboard temperature	1000	K
Diameter of arc impingement spots on melt surface	0.6	m
Arc heat supplied to melt	50	MW
Initial melt temperature	1800	K

Table 2: Model parameters used for the simulations.

temperature of the melt, the resulting heat losses from the surface can be estimated to be in the order of 5 MW.

Simulations of the reference EAF were performed for two scenarios:

- Electromagnetic stirring directed towards the EBT region, using ABB's new EAF-EMS stirrer design,
- Only natural convection, due to the arc heating of the surface.

The calculations were run to simulate 600 s (10 min) of real time, with time averaging of mean flow properties during the last 300 s. The melt is initially at rest, with a uniform initial temperature of 1800 K. The energy equation is solved from the start, with a ramp-up of arc power over the first 60 s. The mixing efficiency of the fully developed flow is assessed by solving for a passive trace scalar during the last 300 s. The trace scalar concentration is initially given a linear vertical profile, with values of 0 and 1 at the bottom and top surfaces, respectively.

Flow patterns and melt velocity

Figure 5 shows the volume-averaged melt speed as a function of time. While natural convection generates melt velocities of only a few centimeters per second, electromagnetic stirring accelerates the melt to an average velocity of about 0.5 m/s. The maximum velocity is about 1 m/s. The curves suggest that the initial transient to reach a developed flow last for 3-4 minutes.

The mean flow pattern created by natural convection is illustrated in Figure 6, which shows velocity vectors in two vertical planes through the centre of the furnace. The simulation predicts a severely stratified flow, with only weak flow in the rounded bottom half of the melt volume. However, natural convection flows are very sensitive; the stratification will certainly be less pronounced in the real process, where the flow pattern will break up due to surface instabilities, oxygen lancing, pieces of scrap and other disturbances. Nevertheless, this is clearly a flow prone to thermal stratification and poor mixing in the bottom of the furnace.

The flow pattern with electromagnetic stirring is illustrated in Figure 7. Electromagnetic stirring creates a strong global circulation in the furnace, also in the EBT region. The flow in the horizontal cross-section is slightly asymmetric; the flow evolves slowly, and the mean velocity pattern has not yet stabilized at the end of the simulation.

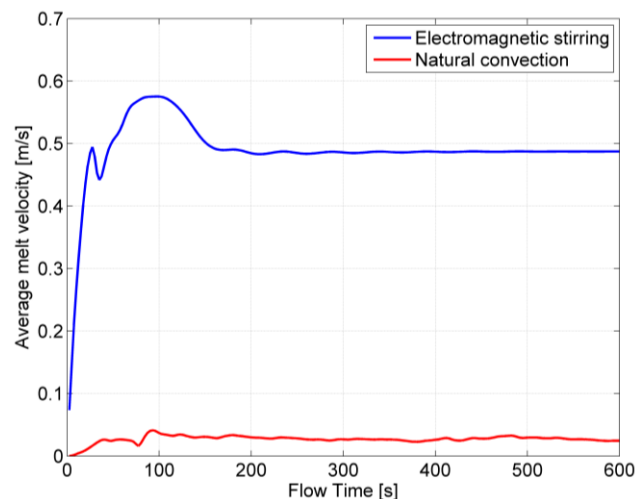


Figure 5: Development of average speed in the melt during the simulation.

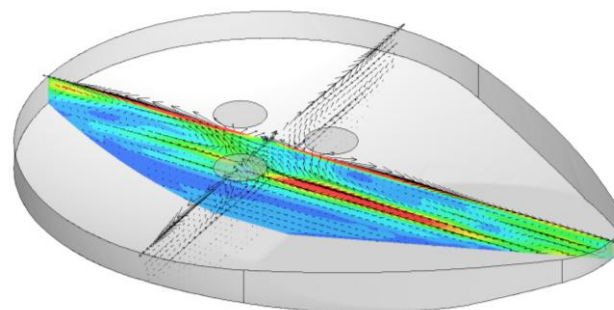


Figure 6: Mean flow pattern created by natural convection (no stirring). The flow is stratified near the middle of the furnace.

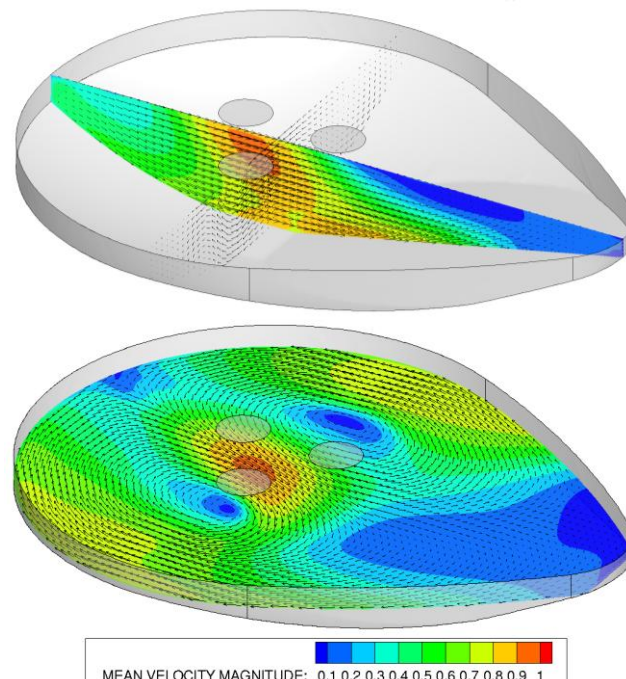


Figure 7: Mean flow pattern created by electromagnetic stirring. Vertical planes (top) and horizontal plane 27 cm below surface (bottom).

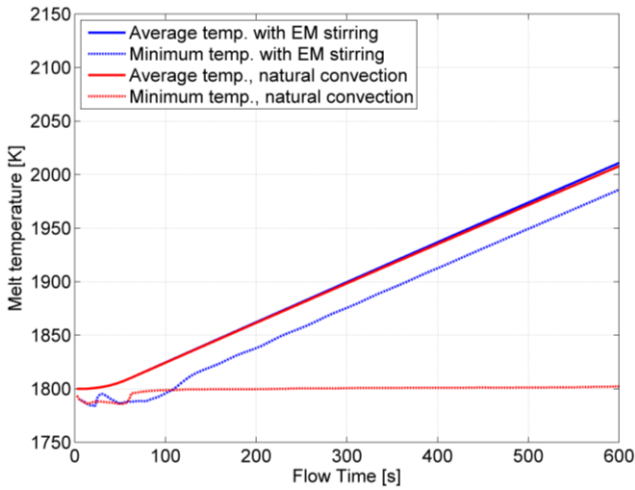


Figure 9: Difference between minimum and average temperatures in the melt with and without electromagnetic (EM) stirring.

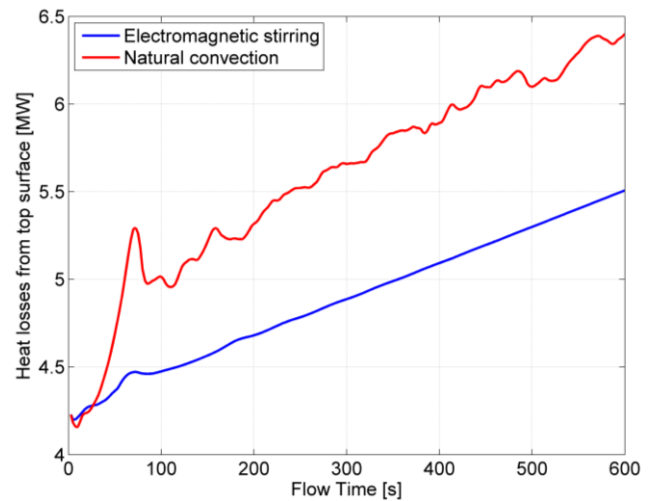


Figure 8: Heat loss across the top boundary, representing the slag layer and the heat transfer to the freeboard.

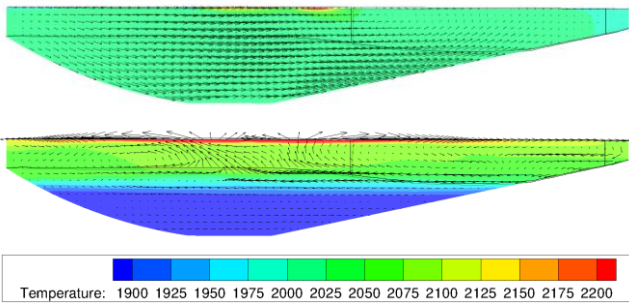


Figure 10: Contours of instantaneous temperature (K), at $t=600$ s, and mean velocity vectors (vectors are not the same scale) for electromagnetic stirring (top) and natural convection (bottom).

Heat transfer and temperatures

As shown in Figure 9, the average melt temperature increases linearly beyond the initial ramping of power, for both cases. With electromagnetic stirring, the minimum temperature lags less than a minute behind the average temperature, despite the rapid heating. This is an indication of the good mixing of the melt. For the case of natural convection, however, the thermal stratification causes the minimum temperature to remain close to the initial.

The difference in temperature distributions is illustrated also by the contour plots in Figure 10, showing the mean temperature distribution in a vertical cross-section at $t=600$ s. The temperature is very homogeneous with electromagnetic stirring. With only natural convection we have a region in the bottom with cold melt, while a layer near the surface is at least 100 K hotter than the melt in average. The almost stagnant condition in the bottom is linked to the thermal stratification, but the problem of super-heating of the surface is related more to the very weak circulation in general; this would remain a problem, even if stratification is broken.

The super-heating of the surface in the absence of stirring is reflected also in the heat losses across the slag layer; see Figure 8, showing the heat losses from the top boundary as a function of time. Electromagnetic stirring reduces the melt surface temperature, reducing the heat losses by 0.6-0.9 MW, or about 15%. The smoothness of the blue curve, compared to the red, suggests that stirring also significantly reduces the temperature fluctuations in the surface layer.

Mixing efficiency

Already the temperature distributions discussed in the previous section give a good feeling for the mixing efficiency of the two flows. A more direct way to look at the mixing efficiency is to solve for a passive trace scalar. This approach comes close to our ongoing efforts to include simplified modeling of key chemical reactions, as they are largely controlled by mass transfer to and from the metal-slag interface.

In the present example we start solving the scalar transport equation after 300 s, when the flow is well developed. The scalar is initially given a linear vertical profile with a value of 1 at the surface and 0 at $Z=0$ (the cut-off bottom of the furnace is located at $Z=0.05$ m, so that the minimum initial value is around 0.05).

Figure 11 shows the evolution of maximum and minimum trace scalar concentrations over time, starting at $t=300$ s. With electromagnetic stirring, the trace scalar is almost perfectly homogenized after about two minutes. With only natural convection the mixing is still poor at the end of the simulation. As before, this is due to the thermal stratification of the melt flow.

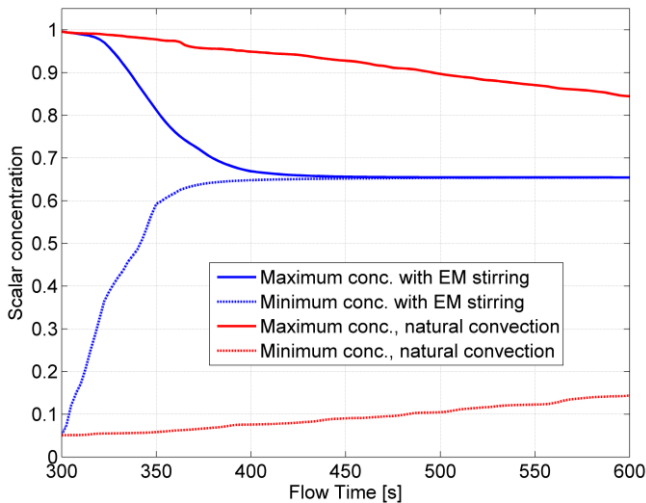


Figure 11: Difference between minimum and maximum trace scalar concentrations with and without electromagnetic (EM) stirring.

Conclusions

Even though the EAF batch process is exceedingly complex to model in complete detail, numerical simulation is an excellent tool for studying separate aspects of the process. The simulation models help us predict the benefits of electromagnetic stirring and optimize the way an electromagnetic stirrer is operated in different stages of the batch process.

In our examples we have highlighted how electromagnetic stirring gives a more than ten-fold increase of the melt flow velocity, compared to natural convection. As a consequence, the span between maximum and minimum temperatures in the melt can be dramatically reduced. This helps avoiding cold regions in the furnace and reduces super-heat of the melt surface. Forced convection also strongly increases the heat transfer between melt and solids, and thus accelerates melting of large pieces of scrap.

A reduced super-heat of the melt surface is shown to reduce heat losses to the freeboard, but a greater gain in energy efficiency probably lies in the possibility to stop heating earlier in the batch without risk of freezing in the bottom, when the temperature distribution is even.

The electromagnetic stirrer provides efficient mixing and homogenization of species concentrations. Together with the even temperature distribution this will improve efficiency and controllability of the chemical reactions in the metal-slag interface. In particular, lower surface temperatures and efficient mixing will lower the iron-oxide content of the slag and increase the yield.

Acknowledgements

We acknowledge valuable input and comments from our colleagues at ABB Metallurgy, Jan-Erik Eriksson and Hongliang Yang, as well as assistance from our thesis student Niloofar Arzpeyma with some of the calculations.

References

- [1] ANSYS FLUENT User's Guide, Release 13.0, Nov. 2010
- [2] Sand, U.; Yang, H.; Eriksson, J-E.; Bel Fdhila, R.; Steel Research Int., Vol. 80, Issue 6, 2009, p. 441-449
- [3] Szekely, J.; McKelliget, J.; Choudhary, M.; Heat transfer, fluid flow and batch circulation in electric arc furnaces and DC plasma furnaces; Ironmaking and Steelmaking, 10(4), 1983, p. 169-179
- [4] Gonzalez, O. J. P.; Ramirez, M.; Conejo, A. N.; effect of arc length on fluid flow and mixing phenomena in AC electric arc furnaces; ISIJ International, Vol. 50, 2010, p. 1-8.